Journal of Neurochemistry

JOURNAL OF NEUROCHEMISTRY | 2013 | 127 | 819–836 doi: 10.1111/jnc.12440

ORIGINAL ARTICLE

The notch signaling pathway: its role in focal CNS demyelination and apotransferrin-induced remyelination

Evangelina Aparicio, Patricia Mathieu, Milagros Pereira Luppi, María Florencia Almeira Gubiani and Ana María Adamo

Department of Biological Chemistry, IQUIFIB (UBA-CONICET), School of Pharmacy and Biochemistry, University of Buenos Aires, C1113AAD, Buenos Aires, Argentina

Abstract

Oligodendroglial damage and demyelination are common pathological features characterizing white matter and neurodegenerative disorders. Identifying the signaling pathways involved in myelin repair through oligodendroglial progenitor maturation is essential for the development of new therapies. This article investigated the role of the Notch signaling pathway in CNS demyelination and apotransferrin-induced remyelination in a focal lysolecithin-induced demyelination model in rats. Notch was found activated in Nestin-expressing neural progenitor cells and in NG2-expressing oligodendroglial precursor cells in the subventricular zone and corpus callosum of lysolecithin-demyelinated rats. Notch activation seemed to be driven by Jagged1, which led to a high expression of downstream gene Hes5 in the subventricular zone of demyelinated rats. Apotransferrin injection induced remyelination, while the injection of the γ-secretase inhibitor reversed this effect. In addition, 24 h after apotransferrin injection, evidence showed Notch activation concomitantly with an increase in F3/contactin levels and the up-regulation of the myelin-associated glycoprotein gene in the subventricular zone and corpus callosum of demyelinated rats. Collected evidence supports the participation of both canonical and non-canonical Notch signaling pathways in demyelination/remyelination. Notch activation was found to trigger Hes5 expression as a consequence of focal demyelination, which might promote oligodendroglial precursor cell proliferation. During apotransferrin-induced remyelination, Notch activation seemed to be mediated by the expression of F3/contactin, which might induce apotransferrin-mediated oligodendroglial maturation.

Keywords: apotransferrin, demyelination, notch signalling, remyelination.

J. Neurochem. (2013) **127**, 819–836.

Demyelination is a pathological process characterized by the loss of myelin around axons. In the CNS, demyelination is generally the consequence of a direct insult to oligodendrocytes (OLs), while remyelination is the process by which myelin sheaths are restored to demyelinated axons, thus resolving functional deficits (Jeffery and Blakemore 1997; Franklin 2002; Liebetanz and Merkler 2006). In the adult brain, NG2-expressing oligodendroglial progenitor cells (OPCs) seem to play a central role in the remyelination process. OLs, derived from neural precursor cells (NPCs) present in the subventricular zone (SVZ), contribute to the remyelination of demyelinated areas in the corpus callosum (CC). In addition, local OPCs distributed throughout the adult CNS are involved in myelin repair (Franklin and Ffrench-Constant 2008).

Remyelination is often inadequate in demyelinating diseases such as multiple sclerosis (MS) and the reasons for the eventual

Received May 7, 2013; revised manuscript received August 7, 2013; accepted August 27, 2013.

Address correspondence and reprint requests to Dr Ana M. Adamo, Department of Biological Chemistry, University of Buenos Aires, Junín 956, C1113AAD, Buenos Aires, Argentina.
E-mail: amadamo@qb.ffyb.uba.ar

Abbreviations used: APC, adenomatous polyposis coli; aTf, apotransferrin; bHLH, basic helix-loop-helix; CC, corpus callosum; CPZ, cuprizone; DAPT, *N*-[*N*-(3,5-Difluorophenalcetyl-L-alanyl)]-*S*-phenylglycine-t-butyl ester; DFX, deferroxamine; DSL, Delta, Serrate/Jagged and Lag-2 ligands; EAE, Experimental Autoimmune Encephalomyelitis; ECL, enhanced chemiluminescence; GAPDH, glyceraldehyde-3-phosphate dehydrogenase; GFAP, glial fibrillary acidic protein; GSA, lectin Griffonia simplicifolia; Hes, Hairy/Enhancer of Split; IHC, immunohistochemistry; IOD, integrated optical density; LPC, lysolecithin; MAG, myelin-associated glycoprotein; MBP, myelin basic protein; MS, multiple sclerosis; Ngn, Neurogenin; NICD, Notch intracellular domain; NPCs, neural progenitor cells; OL, soligodendrocytes; OPCs, oligodendroglial progenitor cells; PBS, phosphate-buffered saline; RT-PCR, real time PCR; SS, sterile saline solution; SVZ, subventricular zone; TBS, Tris-buffered saline; TBST, TBS 0.025% Triton.

failure of repair mechanisms remain unknown. Therefore, the characterization of OPCs and of the mechanisms involved in their proliferation, migration, and differentiation is crucial to the design of strategies to improve remyelination in demyelinating disorders. A very dynamic combination of different transcription factors is expressed during OL differentiation (Nicolay *et al.* 2007). In neuro-epithelial cells, the Delta/Notch signaling pathway regulates the expression of either the neurogenic basic helix loop helix (bHLH) Neurogenin (Ngn) or the oligodendrogliogenic bHLH Olig 2, leading to their differentiation into motoneurons or OPCs, respectively (Park and Appel 2003). Notch is a type I transmembrane receptor which responds to the binding of specific ligands to its extracellular epidermal growth factor-like repeats and consequently undergoes a sequence of two proteolytic cleavages. The first cleavage, by ADAM metalloprotease(s) at site 2 (S2), creates a membrane-tethered intermediate that becomes the substrate for the γ-secretase complex, which, in turn, releases the Notch intracellular domain (NICD). NICD subsequently translocates to the nucleus and activates the transcription of Notch target genes (Kopan and Ilagan 2009) such as the bHLH-type transcriptional repressors known as Hairy/Enhancer of Split (Hes) genes. Upon binding to typical Delta, Serrate/Jagged and Lag-2 ligands, Notch activation maintains the pool of NPCs in their undifferentiated state and enables the generation of OPCs (Artavanis-Tsakonas *et al.* 1999). Both Jagged- and Delta-Notch ligands block OL maturation (Wang *et al.* 1998). Furthermore, NB-3 and F3/contactin, two neural cell adhesion molecules, act as functional Notch ligands participating in OL generation (Hu *et al.* 2003; Cui *et al.* 2004). NB-3 triggers NICD nuclear translocation, promoting oligodendrogenesis from progenitor cells and OPC maturation via Deltex1 (Cui *et al.* 2004).

It was previously shown that a single intracranial injection of apotransferrin (aTf) to 3-day-old rats increases brain myelin content, including proteins and their mRNAs (Escobar Cabrera *et al.* 1994, 1997, 2000). Transferrin regulates myelin basic protein gene transcription (Espinosa de los Monteros *et al.* 1989, 1999) and its action synergizes with that of insulin-like growth factor one (IGF-1), enhancing myelination in myelin-deficient rats (Espinosa-Jeffrey *et al.* 2002). Transgenic mice over-expressing the human transferrin gene show an increase in myelin content very similar to that observed in rats receiving an intracranial injection of aTf (Saleh *et al.* 2003).

Regarding experimental models of demyelination, the addition of cuprizone (bis-cyclohexanone oxalydihydrazone, CPZ) to the diet of adult mice causes massive demyelination in the CNS, particularly in the CC (Suzuki and Kikkawa 1969; Ludwin 1978; Matsushima and Morell 2001). In this field, we demonstrated that the treatment of demyelinated rats with a single aTf (350 ng) injection at the time of CPZ withdrawal induces a marked increase in myelin deposition as compared to the spontaneous remyelination observed in control animals (Adamo *et al.* 2006).

Taking into account our previous results, in this study we evaluated the effects of aTf on CC remyelination in an experimental model of focal demyelination induced by a stereotaxic injection of lysolecithin (LPC). We further investigated the role of the Notch signaling pathway in the demyelination process and characterized the involvement of Notch in aTf-induced remyelination.

Materials and methods

Materials

Rat aTf, bovine serum albumin, paraformaldehyde and Triton X-100 were purchased from Sigma Chemical Co. (St. Louis, MO, USA). The Fluorescent BrainStain Kit was obtained from Molecular Probes (Eugene, OR, USA). The protease inhibitor cocktail was obtained from Roche Diagnostics (GmbH, Mannheim, Germany). LPC, γ-secretase inhibitor *N*-[*N*-(3,5-Difluorophenalcetyl-L-alanyl)]-S-phenylglycine-t-butyl ester (DAPT) were obtained from Calbiochem (Merck KGaA, Darmstadt, Germany). Deferroxamine (DFX) was obtained from Novartis (Ciudad Autónoma de Buenos Aires, Argentina). Antibodies against Notch, NICD and NG2 were from Chemicon (Billerica, MA, USA). The antibody against adenomatous polyposis coli (APC antibody, also known as CC1) was obtained from Calbiochem (Merck KGaA). Antibodies against Nestin and Jagged1 were from Santa Cruz Biotechnology (Santa Cruz, CA, USA). The antibody against F3/contactin was a gift from Dr. K. Watanabe (Nagaoka University of Technology, Department of BioEngineering, Japan). The antibody against glial fibrillary acidic protein (GFAP) was obtained from Dako (Carpinteria, CA, USA) and the biotinylated lectin Griffonia simplicifolia (GSA-1B4) was obtained from Vector Laboratories (Burlingame, CA, USA). Secondary Cy2- and Cy3-conjugated antibodies and the Cy2-conjugated streptavidin were obtained from Jackson Immuno Research Co. Laboratories (West Grove, PA, USA). RNA*later* and RNAqueous-Micro were purchased from Ambion (Foster City, CA, USA). SYBR Green I dye, primers, the High-Capacity cDNA Reverse Transcription Kits, and the TaqMan RT Kit were obtained from Applied Biosystems (Foster City, CA, USA). All other chemicals were analytical grade reagents of the highest purity available.

Animals

A highly in-bred strain of Wistar rats was raised in our own animal facilities. All animal procedures were in accordance with standards outlined in the NIH Guide for the Care and Use of Laboratory Animals. Animals were housed under standard conditions on a normal 12 h light/dark cycle. Focal demyelination was induced in adult Wistar rats of both sexes (50–60 days old). Rats were deeply anaesthetized with a ketamine/xylaxine cocktail (75 mg and 10 mg per kg of body weight, respectively), positioned in a stereotaxic frame and injected 1 μL of 2% LPC in sterile saline solution (SS). The demyelinating agent was injected unilaterally into the CC using the stereotaxic coordinates, 0.5 mm anterior relative to bregma, 1.5 mm mediolateral and 2.5 mm dorsoventral from the surface of the skull, and the needle was kept in place for 5 min to reduce reflux along the needle track. Controls were injected 1 μL of SS. Day 7 after LPC injection was designated as time zero (t0). At t0, animals were injected a single dose of 350 ng of aTf prepared in 1 μL SS while controls were injected 1 μL SS only. Intraventricular injections were

performed in one of the lateral ventricles at the following coordinates: 1 mm posterior relative to bregma, 1.5 mm mediolateral and 3.5 mm dorsoventral from the surface of the skull. After aTf or SS injections, animals were killed at different time points (2, 6 and 24 h, 0, 3, 7 or 23 days depending on the experiment).

To inhibit the Notch pathway, a subgroup of LPC-demyelinated animals received an intraventricular injection of 1 μL of 1 mM DAPT, a γ-secretase inhibitor, 5 min before the injection of aTf. In addition, another group received an intraventricular injection of 10 ng of DFX in 1 μL of SS, 5 min before the injection of aTf, to test whether aTf effects were because of iron or the protein itself. Injections of aTf, DAPT and DFX were all delivered in the hemisphere where demyelination had been induced. For immunohistochemistry (IHC), brains from at least six animals for each experimental condition were excised, processed and frozen at −80°C. For western blot or Real Time PCR (RT-PCR) analyses, CC and SVZ were dissected from the hemispheres either submitted to focal demyelination or injected with SS and then frozen at −80°C. To ensure sufficient amounts of protein and RNA, every western blot and RT-PCR study made it necessary to pool tissue from three animals.

Preparation of tissues and microscopic examination

Rats were deeply anesthetized as described above and perfused transcardiacally with phosphate-buffered saline, pH 7.4 (PBS), followed by 4% (w/v) solution of paraformaldehyde in PBS. The brains were carefully dissected out and post-fixed in the same solution overnight, followed by thorough washing in PBS; then cryoprotection was performed in 15% (w/v) sucrose in PBS for 24 h and 30% (w/v) sucrose for 3 days. The tissue was then frozen and used to obtain 30 μm free-floating coronal sections using a Leica CM 1850 cryotome (Leica Microsystems, Nussloch, Germany). Microscopic observations were done using an Olympus BX50 microscope and photographs were taken with a CoolSnap digital camera. The Image Pro Plus software (version 5.5, Media Cybernetics Inc., Rockville, MD, USA) was used for image analysis. Myelin staining was carried out with a Fluorescent BrainStain Imaging Kit (Molecular Probes, Eugene, OR, USA), which uses FluorMyelin Green to selectively label myelin, and 4′,6-Diamino-2-Phenylindole to stain nuclei.

Immunohistochemistry

Previous to IHC, brain sections were checked for demyelination using a Fluorescent BrainStain Imaging Kit as described above. Cryotome sections were rinsed twice with Tris-buffered saline, pH 7.6 (TBS), followed by TBS 0.025% Triton (TBST) and then blocked for 2 h with a solution containing 5% (w/v) bovine serum albumin in TBS. Incubation with the primary antibodies was done overnight at 4°C. The primary antibodies used were anti-NG2 (1 : 100) to identify OPCs, anti-APC (1 : 100) to detect further differentiated OLs, anti-Nestin (1 : 100) to identify NPCs and anti-NICD (1 : 100) to evaluate Notch signaling activation. In all cases, sections were incubated with a Cy2- or Cy3- conjugated anti-rabbit or anti-mouse secondary antibody for 2 h. After immunostaining, cell nuclei were stained with Hoechst 33342 according to the method of Oberhammer *et al.* 1993. The inflammatory response was analyzed at 7, 14, and 30 days after LPC administration in each experimental group. In this case, free-floating sections were incubated in blocking solution (1% donkey serum, 0.1% Triton in 0.1 M PBS) and incubated overnight with primary antibodies, anti-GFAP (1 : 700) for astrocytes and the GSA-1B4 (1 : 100) for microglial cells (Kaur and Ling 1991). Sections were then incubated with either Cy3-conjugated donkey anti-rabbit antibody (1 : 200) or Cy2-conjugated streptavidin (1 : 200), respectively. Microscopic observations were done in an Olympus BX50 epifluorescence microscope (Olympus, Tokyo, Japan) provided with a Cool-Snap digital camera. The integrated optical density, measured as relative to area, was determined for the different antibodies at each experimental condition in five randomly selected fields of the CC and SVZ. Evaluation of the data was carried out using the Image Pro Plus 5.1 software. To study the colocalization between NICD and NG2 or Nestin, sections were examined by laser confocal microscopy using an Olympus FV 300 microscope (Olympus). Optical sections (Z = 1 μm) of confocal epifluorescence images were acquired sequentially using a 60X (NA, 1.35; digital zoom of 2.2) oil objective. Olympus Fluoview version 4.0a software was used to merge images and orthogonal studies.

Western blot analysis

Tissues were homogenized in 50 mM Hepes buffer (pH 7.4) containing 150 mM NaCl, 0.5 mM EDTA, 2% (v/v) Igepal, phosphatase inhibitors (1 mM sodium pervanadate, 100 μM NaF), and protease inhibitors (1 mM phenylmethylsulfonyl fluoride , 0.5 μg/mL leupeptin, 0.7 μg/mL pepstatin, 40 μg/mL and 1 μg/mL aprotinin). Homogenates were incubated for 30 min on ice and centrifuged at 15 000 *g* for 30 min. The protein content in the samples was measured according to Bradford (Bradford 1976). Sample aliquots containing 50 μg of protein were separated by SDS-PAGE, 10% w/v acrylamide (Laemmli 1970) and then blotted onto polyvinylidene difluoride PVDF membranes. After a 2-h blockade in 5% (w/v) non-fat milk in PBS, membranes were probed overnight at 4°C with the different primary antibodies (NICD 1 : 750; Jagged1 1 : 500, F3/contactin 1 : 1000; Tubulin 1 : 1000). Membranes were subsequently incubated for 90 min at 20°C with the corresponding secondary horseradish peroxidase-conjugated antibody (1 : 10 000). The bands were visualized by enhanced chemiluminescence (ECL plus; Amersham Biosciences, Piscataway, NJ, USA) using a Phosphoimager 840 (GE Healthcare, Piscataway, NJ, USA).

Real-time PCR analysis

Subventricular zone and CC were dissected in RNA*later* solution at 4°C and samples stored at −80°C. Total RNA was isolated with a RNAqueous-Micro Kit. Samples were used for reverse transcription with random hexamer primers, using a High-Capacity cDNA Reverse Transcription Kit and a TaqMan RT Kit. Glyceraldehyde-3-phosphate dehydrogenase (GAPDH) was used as an internal control. RT-PCR was performed using the SYBR Green PCR Master Mix on an Applied Biosystems 7500 Real Time PCR System. Primers were designed using Primer Express Software. The primer sequences were as follows: GAPDH forward: 5′-TGTTCTA GAGACAGCCGCATCTT-3′;

GAPDH reverse: 5′-CACCGACCTTCACCATCTTGT-3′;

Hes 1 forward: 5′-CAGAAAGTCATCAAAGCCTATCATG-3′;

Hes 1 reverse: 5′-ATCAGTGTTTTCAGTTGGCTCAAAC-3′;

Hes 5 forward: 5′-TCCAGAGCTCCAGGCATGG-3′;

Hes 5 reverse: 5′-CCGCAGTCGATTTTTCTCCTT-3′;

MAG forward: 5′-TCCTGGCCACGGTCATCTA-3′;

MAG reverse: 5′-CACACCAGTACTCCCCATCGT-3′.

Raw data from at least three independent experiments were used to determine the relative expression levels of each transcript by employing the comparative C_T method. In order to use the $\Delta\Delta C_T$ method to calculate the fold-differences in gene expression between samples, a validation experiment was done to determine that the efficiency of the target amplification and the efficiency of the reference (GAPDH) amplification are approximately equal. The amount of target, normalized to an endogenous reference and relative to a calibrator, is given by: $2^{-\Delta\Delta C_T}$ (RQ).

Statistical analysis

Data are presented as the means ± SEM. The statistical analysis was performed either by Student's *t*-test for independent samples or ANOVA (one-way repeated) followed by Tukey's multiple comparison test.

Results

The role of Notch signaling in the regulation of embryonic progenitor cell differentiation has been extensively studied. However, its role in OPC proliferation and differentiation after CNS demyelination and during the remyelination process is still under discussion. The present work examined the role of the Notch signaling pathway in LPC-induced demyelination and in aTf-induced remyelination in adult rats. For this purpose, NICD and Notch ligands were measured by IHC and western blot analyses in the SVZ and CC from animals submitted to demyelination. The expression of Notch downstream signaling genes potentially involved in the proliferation and maturation of OLs was evaluated by RT-PCR.

Notch signaling is activated in the SVZ of demyelinated rats and during aTf-induced remyelination

The SVZ of LPC-demyelinated animals showed evidence of Notch signaling activation. A significant increase in NICD levels was observed upon LPC-induced demyelination both in Nestin and NG2-positive cells present in the SVZ (Fig. 1b). Orthogonal reconstructions of confocal sections in the z-axes confirmed Notch activation (NICD) in Nestin- and NG2-positive cells. In agreement with Notch signaling activation, it is important to highlight the presence of NICD in the nucleus (Fig. 1c). In support of IHC findings, western blot analyses showed a significant increase in NICD in the SVZ of LPC-demyelinated rats, concomitantly with an increase in the level of ligand Jagged1 (Fig. 1d). On the basis of these results, we next studied the expression (RT-PCR) of Hes1 and Hes5, both Notch downstream target genes for the canonical pathway, and myelin-associated glycoprotein (MAG), a gene associated to OL maturation, probably up-regulated by F3/contactin, a non-canonical ligand for Notch. Compared to controls, LPC-demyelinated animals showed a significant increase in SVZ Hes5 mRNA, which is consistent with Notch activation, possibly triggered by Jagged 1, according to western blot results (Fig. 1e). Hes1 and MAG mRNA levels were similar in both groups (Fig. 1e).

We subsequently investigated the effects of an intraventricular injection of aTf on Notch signaling in the SVZ of LPC-demyelinated animals. IHC results showed a significant increase in NICD levels 2 h after aTf injection and a decrease after 6 h (Fig. 2b). Most importantly, LPC-demyelinated animals showed Notch activation (increased SVZ NICD levels) 24 h after aTf injection (Fig. 2b) in NG2- and Nestin-positive cells (data not shown), which is comparable to the activation observed in demyelinated rats 7 days after LPC injection. The injection of DFX immediately before the injection of aTf failed to reverse these changes, which suggests that the protein itself, and not iron, is involved in the effects observed (Fig. 2b). Western blot analyses confirmed the decrease in NICD levels observed through IHC 6 h after aTf injection in demyelinated animals, as well as the increase observed after 24 h (Fig. 2c). Interestingly, F3/contactin, the Notch non-canonical ligand that may be involved in the differentiation and maturation of OPCs, showed a significant increase 24 h after aTf injection (Fig. 2c). On the other hand, neither the intraventricular injection of SS nor the injection of aTf generated significant changes in NICD levels in control animals (data not shown).

Fig. 1 The Notch signaling pathway is activated in the Subventricular zone (SVZ) by lysolecithin (LPC)-demyelination. (a) Notch activation was evaluated in the SVZ 7 days after Sterile saline solution (SS) or LPC injection into the corpus callosum (CC) (t0). (b) Immunohistochemistry (IHC) for the Notch signaling pathway activation marker Notch intracellular domain (NICD) (red), Oligodendroglial progenitor cell (OPC) marker NG2 (green), neural progenitor cell (NPC) marker Nestin (green) and merge (red/green) in SVZ of control (C) and LPC-demyelinated animals (LPC). Scale bar, 200 μm. After quantifications, values were expressed as the ratio integrated optical density (IOD) units/area (μm^2). Each data point represents the mean ± SEM of three independent experiments performed in triplicate. (c) Images display single optical sections of NICD (red), NG2 (green) and Hoechst (blue) or NICD (red), Nestin (green) and Hoechst (blue), scale bar 50 μm. Their overlays and orthogonal reconstructions of confocal sections in the z-axes at the level indicated by the yellow lines are shown on the right panel of each example for control (C) and LPC-demyelinated rats (LPC), scale bar 20 μm. (d) Western blot analyses for NICD and ligand Jagged1 in the SVZ of control (C) and LPC-demyelinated animals (LPC) at t0 (0). After densitometric analyses, protein levels were normalized per tubulin content and expressed as means ± SEM of three independent experiments. (e) Quantitative real time PCR (RT-PCR) analyses of Hes1, Hes5, and myelin-associated glycoprotein (MAG) genes in SVZ of control (C) and LPC-demyelinated animals (LPC) at t0 (0). Values are expressed as RQ and values for LPC animals are considered in reference to those of control rats. Results are presented as means ± SEM of four independent experiments performed in triplicate. Significant differences: $^{**}p < 0.01$ and $^{***}p < 0.001$.

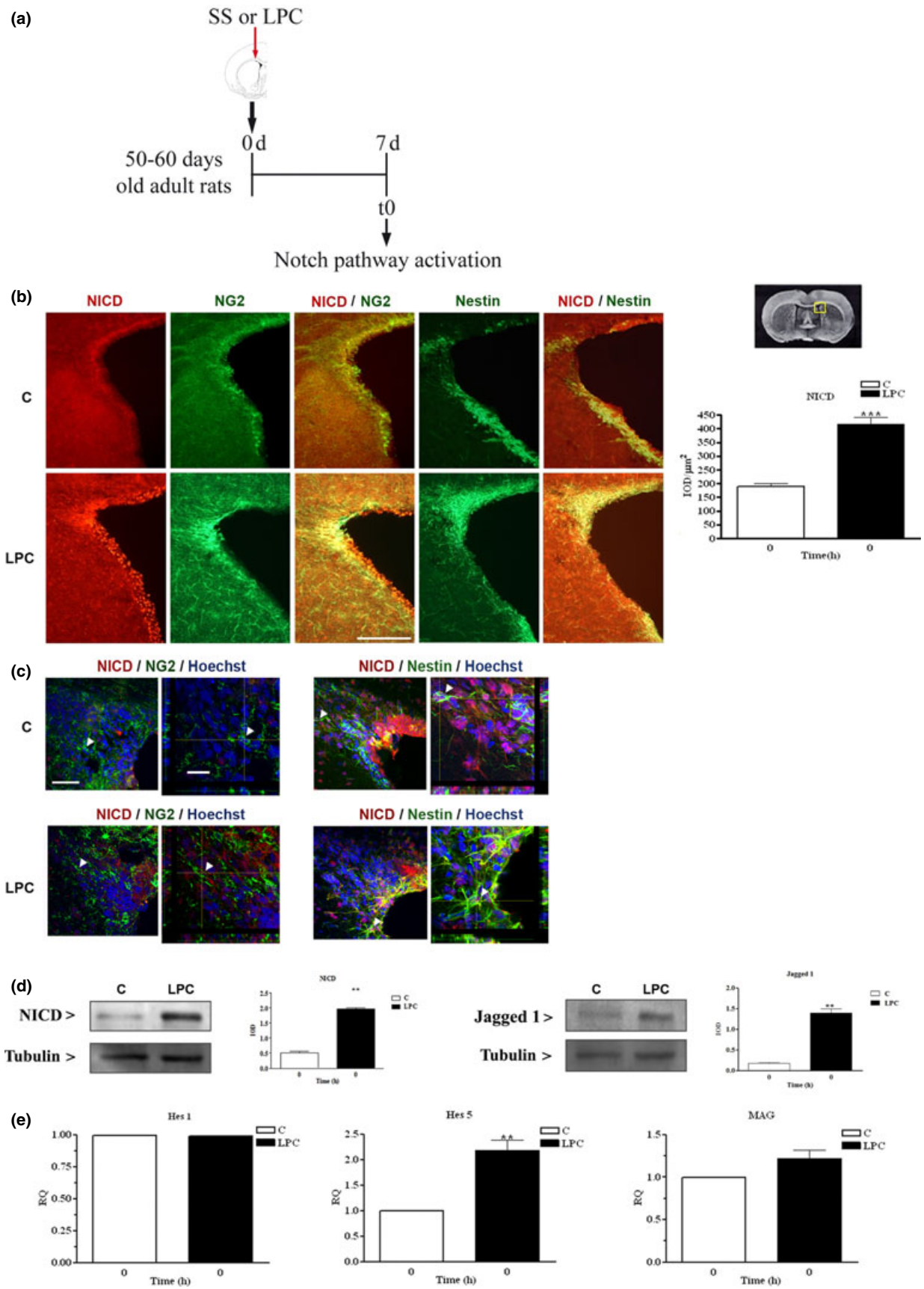
(a)
SS or LPC
0 d
7 d
50-60 days
old adult rats
t0
Notch pathway activation
(b)
NICD
NG2
NICD / NG2
Nestin
NICD / Nestin
C
LPC
NICD
C
LPC
IOD/µm²
Time (h)
(c)
NICD / NG2 / Hoechst
NICD / Nestin / Hoechst
C
LPC
(d)
C
LPC
NICD >
Tubulin >
Jagged 1 >
(e)
Hes 1
Hes 5
MAG
RQ
Time (h)

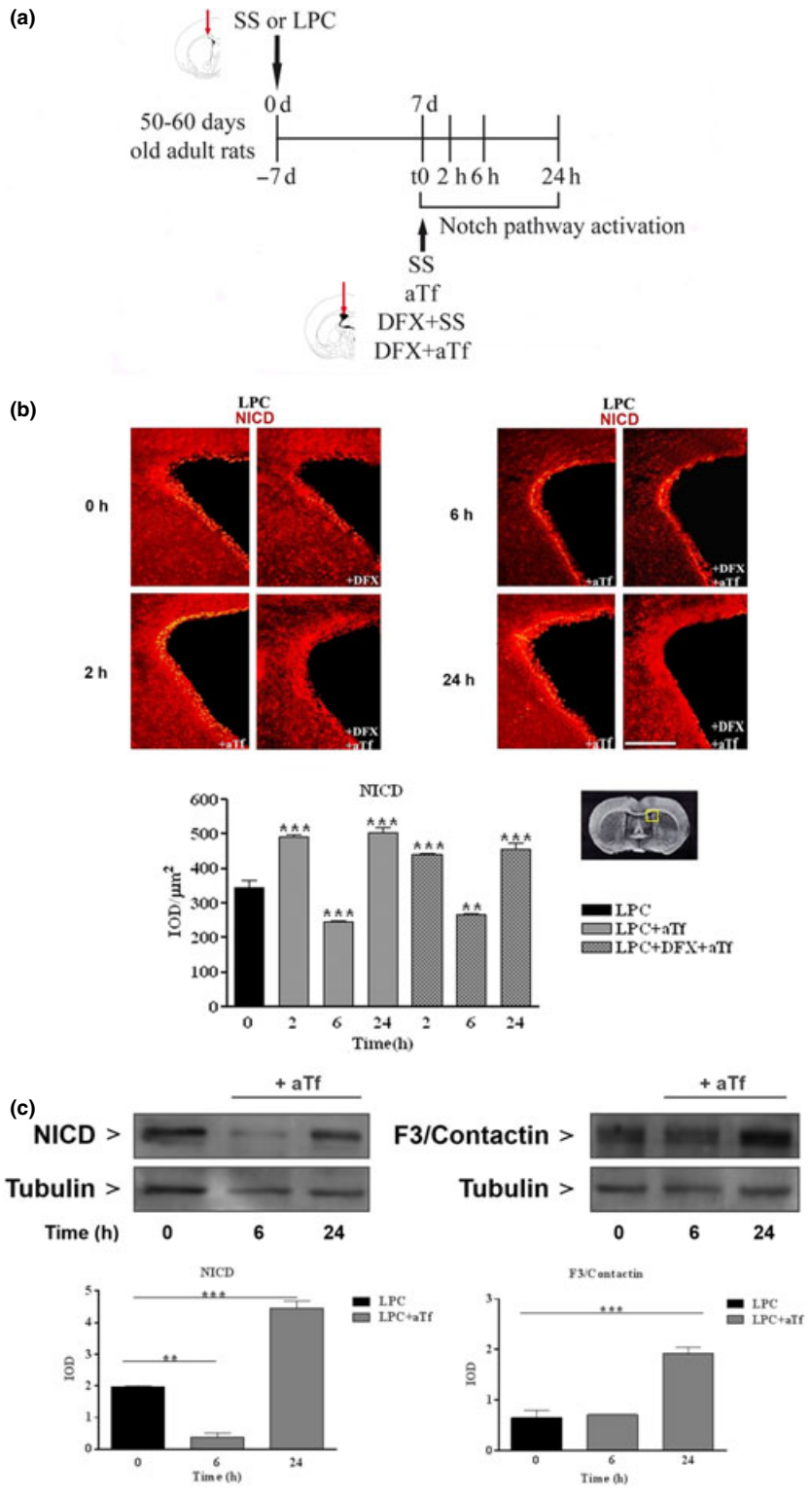

Fig. 2 Characterization of Notch signaling pathway in the Subventricular zone (SVZ) of lysolecithin (LPC)-demyelinated animals after aTf injection. (a) Notch activation was evaluated in the SVZ 7 days after Sterile saline solution (SS) or LPC injection into the corpus callosum (CC) (t0) and 2, 6, and 24 h after the injection of SS, aTf (+aTf), DFX + SS (+DFX), or DFX+aTf (+DFX, +aTf) into the lateral ventricle. (b) Immunohistochemistry (IHC) for Notch signaling pathway activation marker Notch intracellular domain (NICD) (red), in SVZ of LPC-demyelinated rats at 0, 2, 6, and 24 h post-aTf injection (+aTf), in the presence (right column) or absence (left column) of DFX (+DFX). Scale bar, 200 μm. After quantifications, values were expressed as the ratio integrated optical density (IOD) units/area (μm^2). Each data point represents the mean ± SEM of three independent experiments performed in triplicate. (c) Western blot analyses for NICD and non-canonical ligand F3/contactin in SVZ of LPC-demyelinated animals at t0, 6 and 24 h after aTf injection. After densitometric analyses, protein levels were normalized per tubulin content and expressed as means ± SEM of three independent experiments. Significant differences: $^{**}p < 0.01$ and $^{***}p < 0.001$.

With these results, we studied the possible changes induced by the injection of aTf in the expression of Hes1, Hes5, and MAG in the SVZ of LPC-demyelinated and control animals (Fig. 3). Neither control animals submitted to aTf treatment nor control animals injected with SS exhibited significant changes in the expression pattern of these genes (Fig. 3a). However, LPC-demyelinated rats injected with SS suffered a significant decrease in the

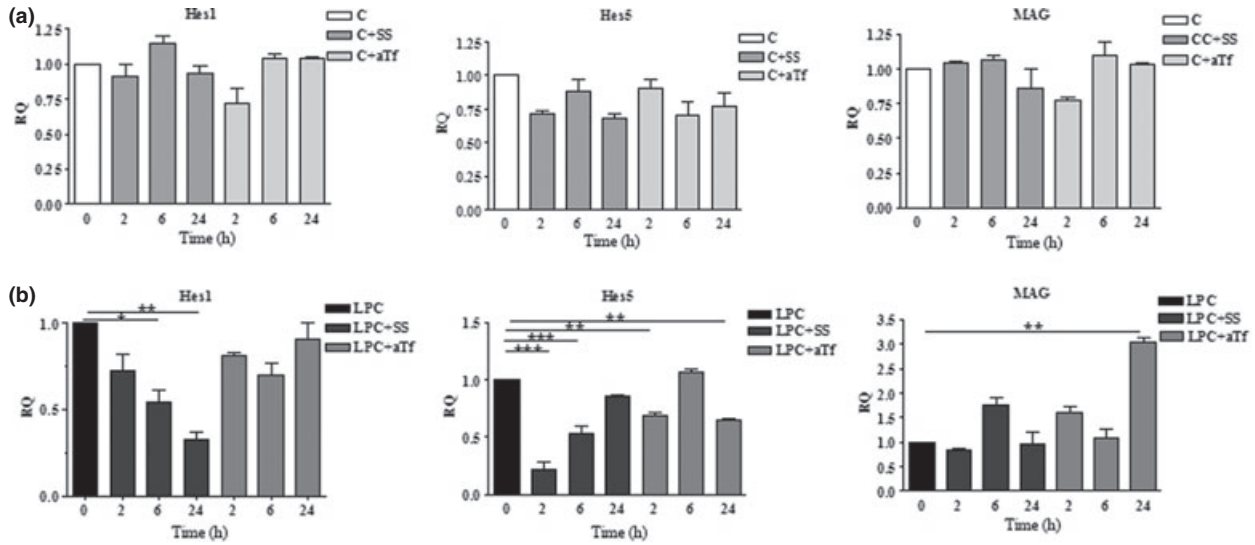

Fig. 3 Relative quantification of Notch signaling target genes Hes1, Hes5, and myelin-associated glycoprotein (MAG) in Subventricular zone (SVZ) of C and lysolecithin (LPC)-demyelinated animals. (a) quantitative real time PCR (RT-PCR) analyses of Hes1, Hes5, and MAG transcripts in SVZ of control animals (C), control animals injected with Sterile saline solution (SS) (C+SS) and control animals injected with aTf (C+aTf). (b) quantitative RT-PCR analyses of Hes1, Hes5, and MAG genes in SVZ of LPC-demyelinated animals (LPC), LPC-demyelinated animals injected with SS (LPC+SS) and LPC-demyelinated animals injected with aTf (LPC+aTF). Both C and LPC animals were evaluated 0, 2, 6, and 24 h post-injection. Values are expressed as RQ. C + SS and C+aTf values at the different times are considered in reference to those of C rats at t0. LPC + SS and LPC + aTf values at different times are considered in reference to those of LPC at t0. Results are presented as means ± SEM of three independent experiments performed in triplicate. Significant differences: $*p < 0.05$, $**p < 0.01$ and $***p < 0.001$.

expression of Hes1 and Hes5 and no changes in the expression of MAG. Although the injection of aTf did not affect the expression of Hes1 at the times analyzed, it did trigger a significant decrease in Hes5 after 2 and 24 h and, most relevant, it triggered a significant increase in MAG transcript levels after 24 h (Fig. 3b). The increase in the levels of F3/contactin 24 h post aTf injection (Fig. 2c) is in line with these results and suggests that Notch signaling activation might be triggered by this non-canonical ligand.

Notch signaling is activated in the CC of demyelinated rats and during aTf-induced remyelination

We subsequently studied the response of the Notch signaling pathway in the CC, the area where focal demyelination is induced by LPC.

In the CC of LPC-treated animals and as a consequence of demyelination, the activation of the Notch signaling pathway was evidenced by an increase in NICD levels (Fig. 4b). As observed in Fig. 4c (control) and 4d (LPC), orthogonal reconstructions of confocal sections in the z-axes showed Notch activation (NICD) in NG2-positive cells of LPC-demyelinated rats. In agreement with Notch signaling activation, it is important to highlight the presence of NICD in the nucleus. According to western blot results, Notch activation appears to be triggered by a significant increase in Jagged1 levels (Fig. 4e). The expression of Hes1, Hes5, and MAG genes was subsequently studied in the CC of LPC-demyelinated animals. In spite of Notch activation, possibly driven by Jagged1, we did not observe changes in the expression of Hes1, Hes5, or MAG genes as compared to controls (Fig. 4f).

We then investigated the effects of an intraventricular injection of aTf on Notch signaling in the CC of LPC-demyelinated animals. IHC results show that the injection of aTf caused a significant increase in NICD levels after 2 and 24 h (Fig. 5b), probably driven by F3/contactin, which also showed a significant increase after 24 h in western blot studies (Fig. 5c). The injection of DFX before the injection of aTf did not reverse these results, which again suggests that the protein itself, and not iron, is involved in this effect (Fig. 5b). Having characterized the expression of Hes1, Hes5, and MAG in the CC of LPC-demyelinated animals, we studied the possible changes in the expression of these genes in the CC of control and LPC-demyelinated animals induced by the injection of aTf (Fig. 6). In agreement with results obtained in the SVZ, no modifications were observed in the expression pattern of these genes in control animals treated with aTf or control animals injected with SS (Fig. 6a). However, in LPC-demyelinated animals, the injection of aTf induced a significant increase in the expression of MAG 24 h later, which is consistent with the activation of Notch signaling, possibly driven by F3/contactin (Fig. 6b).

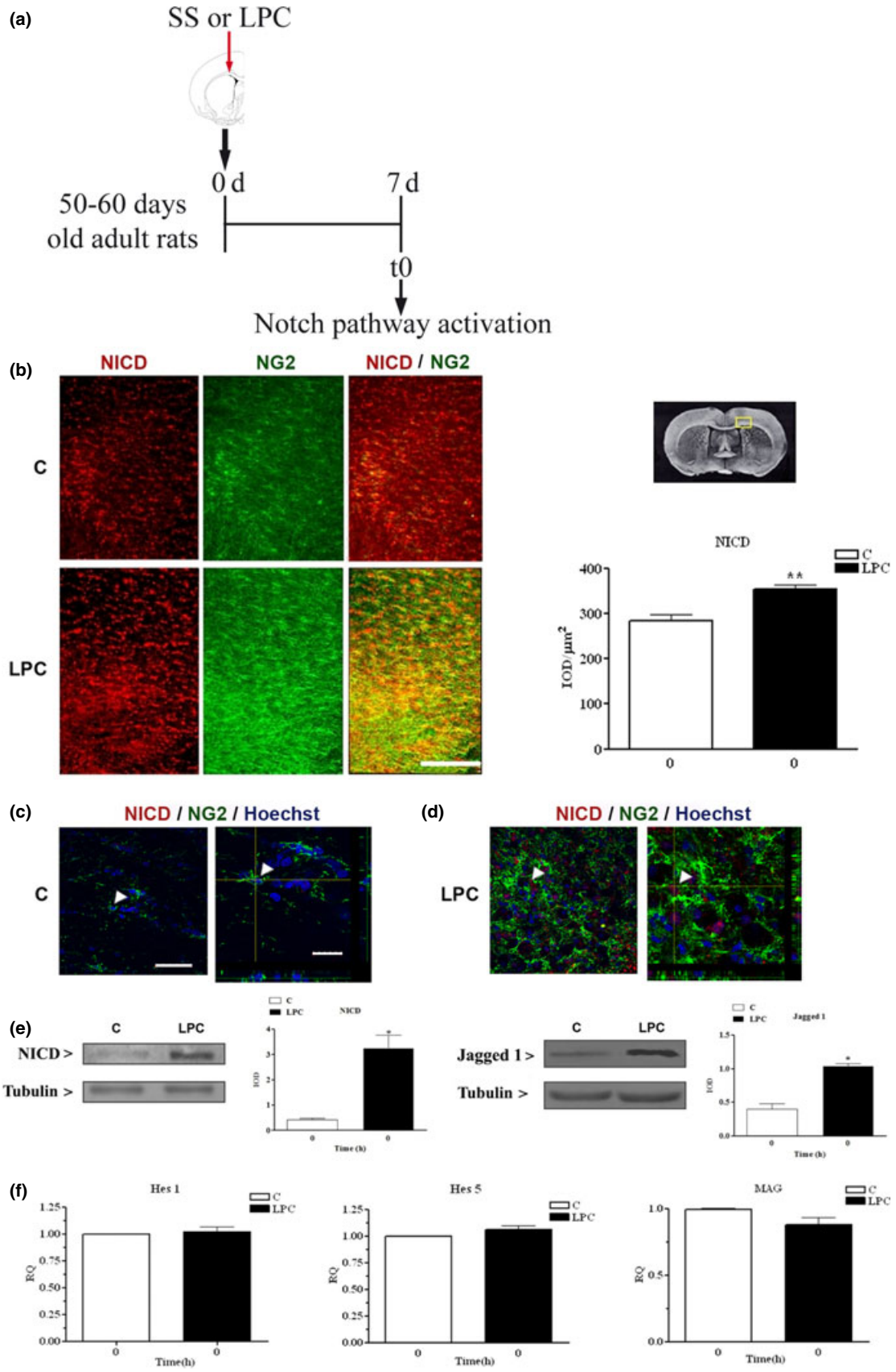
(a)
SS or LPC
0 d
7 d
50-60 days
old adult rats
t0
Notch pathway activation
(b)
NICD
NG2
NICD / NG2
C
LPC
NICD
C
LPC
IOD/μm²
400
300
200
100
0
0
0
(c)
NICD / NG2 / Hoechst
C
(d)
NICD / NG2 / Hoechst
LPC
(e)
C
LPC
NICD >
Tubulin >
NICD
Time (h)
Jagged 1 >
Tubulin >
Jagged 1
(f)
Hes 1
Hes 5
MAG
RQ
Time(h)

Fig. 4 The Notch signaling pathway is activated in the corpus callosum (CC) by lysolecithin (LPC)-demyelination. (a) Notch activation was evaluated in the demyelinated area 7 days after Sterile saline solution (SS) or LPC injection into the CC (t0). (b) Immunohistochemistry (IHC) for Notch signaling pathway activation marker Notch intracellular domain (NICD) (red), Oligodendroglial progenitor cell (OPC) marker NG2 (green) and merge (red/green) in CC of control (c) and LPC-demyelinated animals (LPC). Scale bar, 200 μm. After quantifications, values were expressed as the ratio integrated optical density (IOD) units/area (μm^2). Each data point represents the mean ± SEM of three independent experiments performed in triplicate. (c) Images display single optical sections of NICD (red), NG2 (green) and Hoechst (blue), scale bar 50 μm. Their overlays and orthogonal reconstructions of confocal sections in the z-axes at the level indicated by the yellow lines are shown on the right panel, scale bar 20 μm. (d) Images display single optical sections of NICD (red), NG2 (green), and Hoechst (blue) for LPC-demyelinated rats, scale bar 50 μm. Their overlays and orthogonal reconstructions of confocal sections in the z-axes at the level indicated by the yellow lines are shown on the right panel, scale bar 20 μm. (e) Western blot analyses for NICD and ligand Jagged1 in the CC of control (c) and LPC-demyelinated animals (LPC) at t0 (0). After densitometric analyses, protein levels were normalized per tubulin content and expressed as means ± SEM of three independent experiments. (f) quantitative real time PCR (RT-PCR) analyses of Hes1, Hes5, and myelin-associated glycoprotein (MAG) genes in CC of control (c) and LPC-demyelinated animals (LPC). Values are expressed as RQ and values for LPC animals are considered in reference to those of C rats. Results are presented as means ± SEM of four independent experiments performed in triplicate. Significant differences: $*p < 0.05$ and $**p < 0.01$.

The Notch signaling pathway might be involved in OL development in both SVZ and CC of LPC-demyelinated and aTf-injected animals

The canonical Notch pathway is related to the proliferation of OPCs, while Notch activation by non-canonical ligand F3/contactin might be related to OPC differentiation and OL maturation. We thus studied the population of both NG2-positive OPCs and APC-positive cells (to detect further differentiated OLs) in the SVZ and CC of control and LPC-demyelinated animals at t0 (7 days after LPC injection) and 3 days after the injection of SS or aTf, in the presence or absence of the γ-secretase inhibitor. These studies showed a significant increase in the population of NG2-positive OPCs and no significant changes in the number of APC-positive cells in the SVZ or CC of LPC-demyelinated animals as compared to controls (Figs 7b and 8b).

The injection of aTf induced an increase in the APC-positive population to the detriment of NG2-positive OPCs, both in the SVZ and CC. Consistently with our hypothesis about Notch signaling participation in OPC proliferation and/or differentiation, γ-secretase inhibitor DAPT blocked the effect of aTf, rendering NG2-positive and APC-positive populations unchanged as compared to LPC-demyelinated rats receiving only DAPT (Figs 7b and 8b).

To corroborate that the γ-secretase inhibitor had actually blocked Notch activation, we measured the levels of NICD and the expression of downstream genes both in the SVZ and CC of LPC-demyelinated animals. Results showed an inhibition of the increase in NICD levels in both areas in the LPC group. In addition, DAPT blocked the activation of the Notch signaling pathway observed after aTf injection. Accordingly, the γ-secretase inhibitor prevented the expression of Hes 1, Hes 5 and MAG (Figs 7c, d and 8c, d).

Also and most importantly, we confirmed the promyelinating effect of aTf in LPC-demyelinated animals and evaluated the possible participation of the Notch signaling pathway in this effect. This evaluation was conducted through histological analyses using myelin-specific staining 7 days after aTf or SS injection. Results show that, unlike SS, aTf accelerated myelin deposition in the lesion area in the CC, and that the inhibition of Notch signaling activation through DAPT injection (Fig. 8e) reversed this promyelinating effect. With these results and in order to evaluate astrocytic and microglial response to demyelination and during the remyelination process, we evaluated the inflammation response 7, 14, and 30 days after SS or LPC injection and 7 and 23 days after the injection of aTf, the γ-secretase inhibitor DAPT or DAPT + aTf. Microglial activation was detected by GSA-lectin staining in the CC ipsilateral to the toxin injection. GSA-positive cells with activation stages 2, 3, and 4 (Kreutzberg 1996) were observed in the LPC injection site (Fig. 9b). The lectin-positive cells were not only restricted to the LPC injection site but also observed in the entire CC at each experimental time and regardless of treatment. Activation stage 4 was detected mainly near the injection site. In addition, GFAP-positive astrocytes were detected in the injection area regardless of treatment or time point studied (Fig. 9b and d).

Discussion

The study of intracellular signals involved in remyelination is crucial to understanding this important process and designing future strategies aimed at myelin repair and regeneration. MS, which is one of the most frequent neurological disorders affecting young adults, is characterized by the destruction of CNS myelin as a consequence of persistent inflammation in the brain and spinal cord (Lassmann *et al.* 2007). Histologically, MS is characterized by foci of CNS inflammation, demyelination and axonal damage. Demyelinating disorders are characterized by neurodegeneration as the consequence of remyelination failure. The mechanisms underlying this failure are still to be fully elucidated, although special attention is frequently drawn to the fact that MS lesions

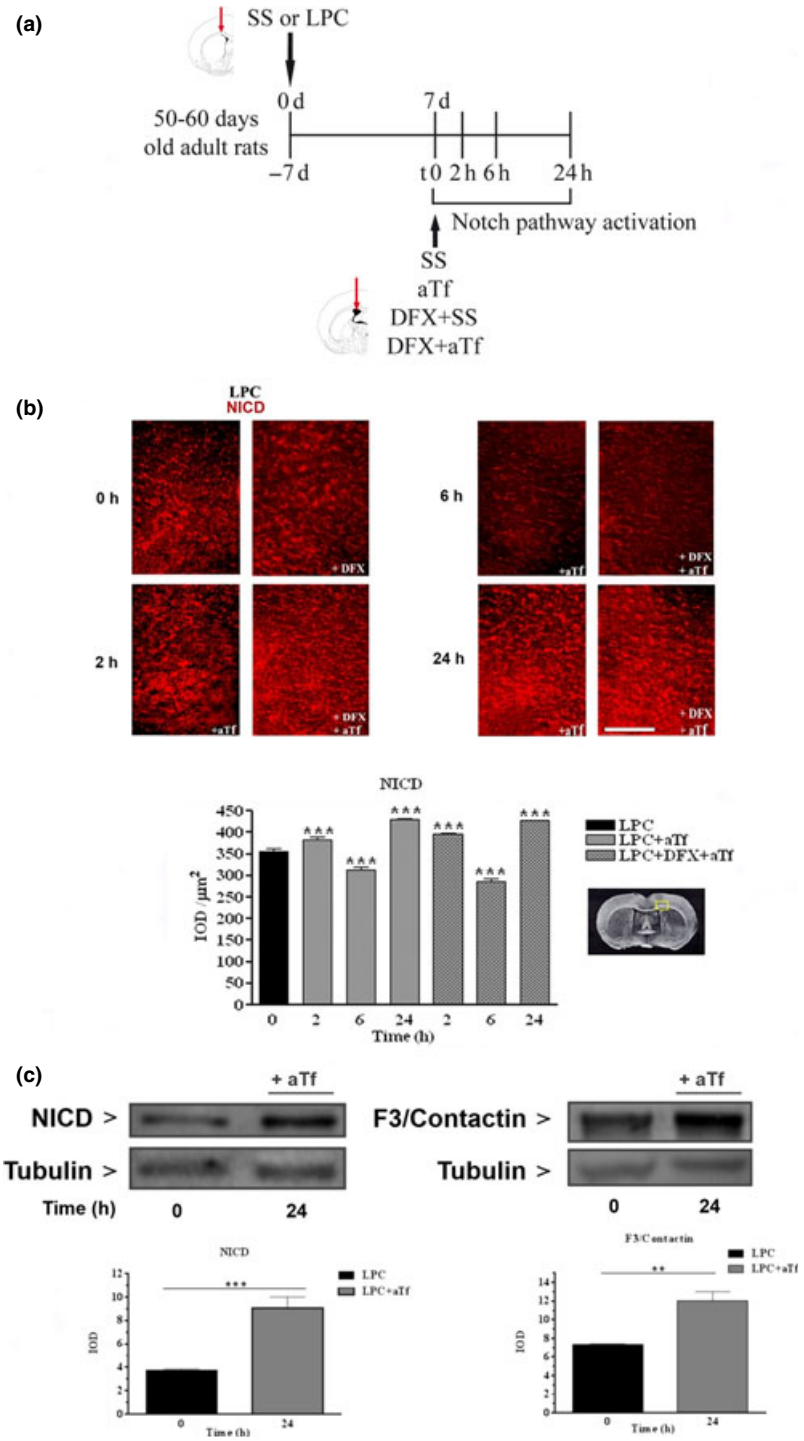

Fig. 5 Characterization of Notch signaling pathway in the corpus callosum (CC) of lysolecithin (LPC)-demyelinated animals after aTf injection. (a) Notch activation was evaluated in the demyelinated area 7 days after Sterile saline solution (SS) or LPC injection into the CC (t0) and 2, 6, and 24 h after the injection of SS, aTf (+aTf), DFX+SS (+DFX) or DFX+aTf (+DFX, +aTf) into the lateral ventricle. (b) Immunohistochemistry (IHC) for Notch signaling pathway activation marker Notch intracellular domain (NICD) (red) in the CC of LPC-demyelinated rats 0, 2, 6, and 24 h after aTf injection (+aTf), in the presence (right column, +DFX) or absence (left column) of deferroxamine (DFX). Scale bar: 200 µm. After quantifications, values were expressed as the ratio integrated optical density (IOD) units/area (μm^2). Each data point represents the mean ± SEM of three independent experiments performed in triplicate. (c), Western blot analyses for NICD and non-canonical ligand F3/contactin in the CC of LPC-demyelinated animals at t0 and 24 h after aTf injection. After densitometric analyses, protein levels were normalized per tubulin content and expressed as means ± SEM of three independent experiments. Significant differences: $^{**}p < 0.01$ and $^{***}p < 0.001$.

contain numerous OPCs which have the potential capacity to myelinate but which fail to differentiate into mature OLs. On this basis, and considering that the remyelination process might recapitulate a series of events associated with developmental myelination (Miller and Mi 2007), this article investigates the role of canonical and non-canonical Notch1 signaling in endogenous OPC proliferation and/or maturation during demyelination and aTf-induced remyelination.

Oligodendrocytes are the myelinating cells of the CNS, most of which develop during embryogenesis and early postnatal life from select periventricular germinal areas (Warf *et al.* 1991; Timsit *et al.* 1995; Rowitch 2004). OPCs derived from ventricular precursors migrate either tangentially or radially to colonize restricted areas of the brain depending on their site of origin (Thomas *et al.* 2000). Most important, OLs continue to be generated in the adult brain

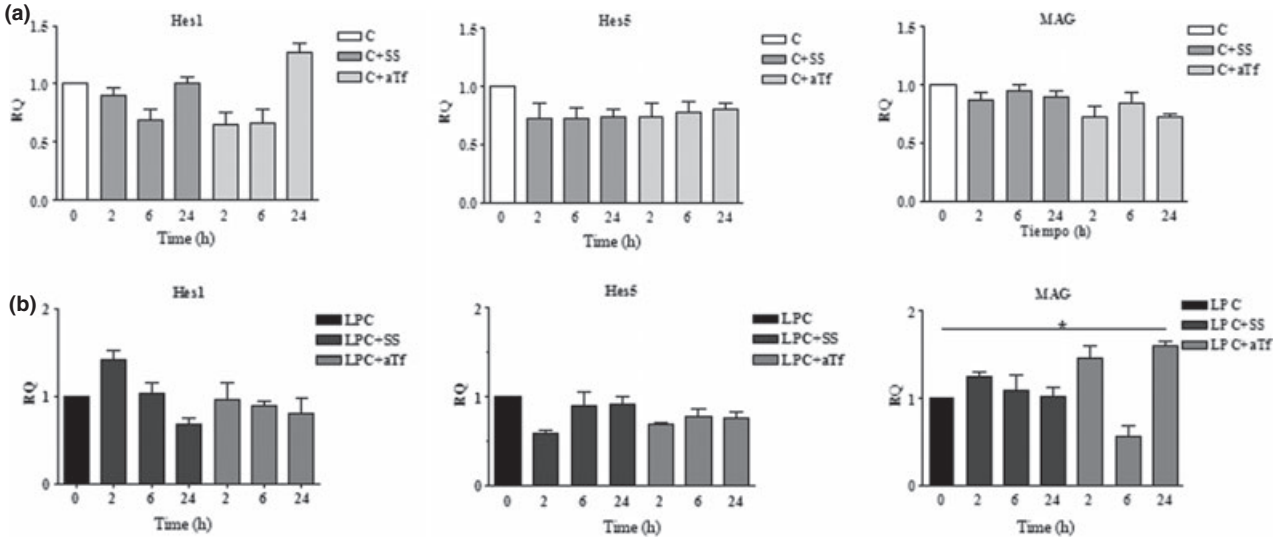

Fig. 6 Relative quantification of Notch signaling target genes Hes1, Hes5, and myelin-associated glycoprotein (MAG) in corpus callosum (CC) of C and lysolecithin (LPC)-demyelinated animals. (a) quantitative real time PCR (RT-PCR) analyses of Hes1, Hes5, and MAG transcripts in CC of control animals (c), control animals injected with Sterile saline solution (SS) (C+SS) and control animals injected with aTf (C+aTf). (b) quantitative RT-PCR analyses of Hes1, Hes5, and MAG genes in CC of LPC-demyelinated animals (LPC), LPC-demyelinated animals injected with SS (LPC+SS) and LPC-demyelinated animals injected with aTf (LPC+aTF). Both C and LPC animals were evaluated 0, 2, 6, and 24 post-injection. Values are expressed as RQ. C+SS and C+aTf values at the different times are considered in reference to those of C rats at t0. LPC+SS and LPC+aTf values at different times are considered in reference to those of LPC at t0. Results are presented as means ± SEM of three independent experiments performed in triplicate. Significant differences: $*p < 0.05$.

(Prineas and Connell 1979; Kaplan and Hinds 1980; McCarthy and Leblond 1988) and are considered to be responsible for remyelination in demyelinating disorders (Chari and Blakemore 2002). Adult OPCs have to be recruited to the demyelinated areas, where they can differentiate into mature OLs with the ability to generate myelin. Therefore, identifying the signaling pathways involved in the complex process of remyelination is highly relevant in the search for pharmacological agents that stimulate endogenous adult OPC maturation.

In addition to the demyelinating action of CPZ demonstrated *in vivo* in mice (Matsushima and Morell 2001), in previous work we have shown that 0.6% (g/g diet) CPZ, fed to weaning Wistar rats for 2 weeks, causes substantial damage to CNS myelin. After CPZ-induced demyelination, treatment with a single intracranial injection of aTf at the time of CPZ termination improves remyelination (Adamo *et al.* 2006). In the present work we evaluated whether the Notch1 signaling pathway is involved in the demyelinating process and in aTf-induced remyelination using the focal LPC-induced demyelination model in rats.

Notch1 signaling activation was found in SVZ and CC of LPC-demyelinated animals. In the SVZ, and in agreement with this pathway activation, NICD was observed in the nucleus of Nestin- and NG2-positive cells and appeared to be triggered by Jagged1. Consequently, we found a high expression of downstream gene Hes5. In the CC, LPC-demyelination also induced Notch1 signaling activation in NG2-positive cells, concomitantly with an increase in Jagged1, although Hes1 and Hes5 levels remained unchanged. This result can be explained in different ways. Firstly, the remyelination process may be already under way by the time of the experiment and different OL populations may thus be present in the CC, such as proliferating, differentiating and mature OLs. Another possible explanation might be the fact that Notch signaling undergoes waves of activation/inactivation driven by different ligands during the process of remyelination. This might be connected to the fact that Notch cleavage is heterogeneous in terms of the γ-secretase cleavage site and that NICD fragments having an N-terminal serine/leucine have a shorter half-life than those with N-terminal valine, which might in turn affect Notch signaling lifespan (Tagami *et al.* 2008). As a third hypothesis, Notch activation may trigger the expression of other genes which were not evaluated in our experiments.

Our results showing Notch1 signaling activation in OPCs and NPCs as a response to demyelination contribute to previous research in the field. For example, during the development of the nervous system, a conditional deletion of RbpjSuh (a DNA-binding protein that interacts with the intracellular domain of activated Notch to regulate transcription) in neural crest cells causes severe defects in gliogenesis (Taylor *et al.* 2007; Gao *et al.* 2009). Also, conditional deletion of Notch1 in the cerebellum causes premature

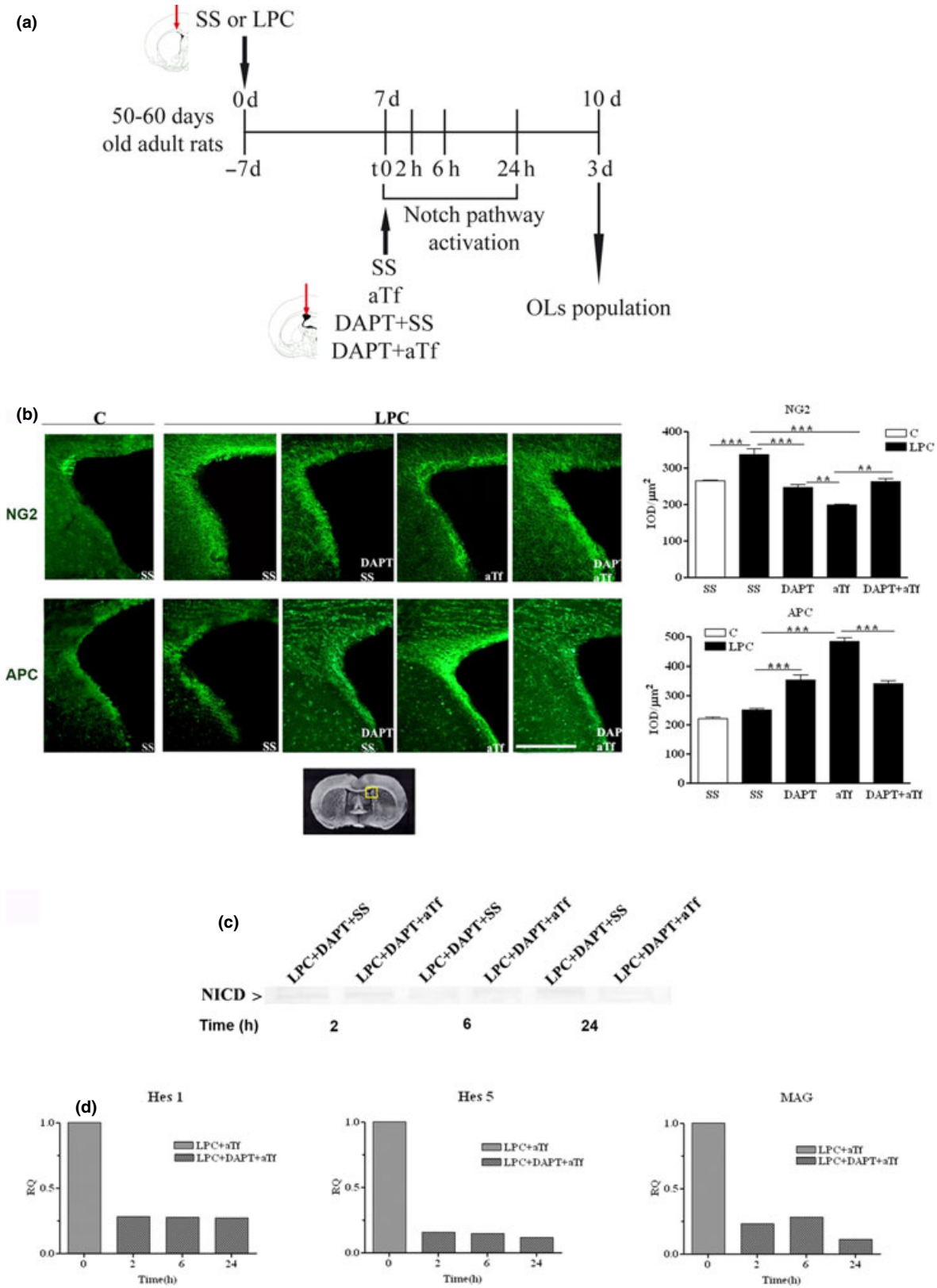
(a)
SS or LPC
0 d
7 d
10 d
50-60 days
old adult rats
–7d
t0 2 h 6 h 24 h
3 d
Notch pathway
activation
SS
aTf
DAPT+SS
DAPT+aTf
OLs population
(b)
C
LPC
NG2
APC
SS
DAPT
aTf
NG2
IOD/μm²
C
LPC
SS
SS
DAPT
aTf
DAPT+aTf
APC
IOD/μm²
(c)
LPC+DAPT+SS
LPC+DAPT+aTf
NICD >
Time (h)
2
6
24
(d)
Hes 1
Hes 5
MAG
RQ
LPC+aTf
LPC+DAPT+aTf
Time(h)

Fig. 7 The changes in NG2-expressing Oligodendroglial progenitor cells (OPCs) and adenomatous polyposis coli (APC)-expressing differentiated oligodendrocytes (OLs) in Subventricular zone (SVZ) of lysolecithin (LPC)-demyelinated rats, induced by aTf injection, are reversed by the γ-secretase inhibitor. (a) OL populations were evaluated in the SVZ of control and LPC-treated rats 3 days after the injection of Sterile saline solution (SS) (SS), aTf (aTf), DAPT+SS (DAPT, SS) or DAPT+aTf (DAPT, aTf) into the lateral ventricle. The inhibition of the Notch signaling pathway was evaluated 2, 6, and 24 h after DAPT+SS or DAPT+aTf injection. (b) Immunohistochemistry (IHC) for NG2-expressing OPCs (green) and APC-expressing differentiated OLs (green) in SVZ of control (C) and LPC-demyelinated animals (LPC) at t0 (SS) and 3 days after SS (SS), DAPT+SS (DAPT, SS), aTf (aTf) and DAPT+aTf (DAPT, aTf). Scale bar: 200 μm. After quantifications, values were expressed as the ratio integrated optical density (IOD) units/area (μm^2). Each data point represents the mean ± SEM of three independent experiments performed in triplicate. (c) Western blot analyses for Notch intracellular domain (NICD) in the SVZ of LPC-demyelinated rats 2, 6, and 24 h after DAPT injection with SS (LPC + DAPT + SS) or aTf (LPC + DAPT + aTf). (d) Quantitative real time PCR (RT-PCR) analyses of Notch signaling target genes. Values are expressed as RQ and values for LPC-aTf rats previously injected with DAPT are considered in reference to those of LPC-aTf rats. Results are presented as means ± SEM of three independent experiments performed in triplicate. Significant differences: $^{**}p < 0.01$ and $^{***}p < 0.001$.

neuronal differentiation and subsequent gliogenesis reduction (Lutolf *et al.* 2002). In the spinal cord, Notch signaling participates in the selection between motoneurons and OPCs by regulating the expression of Olig2 and Ngn, in order to promote the generation of OPCs from a progenitor cell pool (Park and Appel 2003).

Regarding the myelin repair process, one of the reasons for remyelination failure in MS lesions is the presence of reactive astrocytes expressing Jagged1 in response to the up-regulation of transforming growth factor-β1. Notch1 and its effector, Hes5, have been found in OPCs of MS lesions, which suggests that the Jagged-Notch pathway might be responsible for inhibiting OPC maturation (John *et al.* 2002). Similarly, the inhibition of γ-secretase in the CNS of Experimental Autoimmune Encephalomyelitis mice blocks the Notch signaling pathway in OLs, producing remyelination, reduction in axonal damage and clinical recovery (Jurynczyk *et al.* 2008).

Taking into account studies showing the role of aTf during myelination (Escobar Cabrera *et al.* 1994; Espinosa de los Monteros *et al.* 1999; Marta *et al.* 2003) and following the recapitulation of stages associated with development, in previous work we studied the effect of aTf during the remyelination process after CPZ-induced demyelination. We demonstrated an increase in the percentage of proliferating NG2/BrdU-positive OPCs in the CC during acute CPZ-induced demyelination. During the remyelination phase, this increase was followed by a decrease in NG2-positive OPCs, which was accompanied by a significant increase in the percentage of APC-positive OLs when CPZ-demyelinated animals received an intracranial injection of aTf. This suggests that improved remyelination induced by aTf is the consequence of acceleration in OPC maturation, followed by an increase in myelin deposition (Adamo *et al.* 2006). In this work, we have found that the injection of aTf also induces an increase in the APC-positive OLs to the detriment of NG2-expressing OPCs, both in the SVZ and CC of LPC-demyelinated animals, while the injection of the γ-secretase inhibitor succeeds in reversing this effect.

On the basis of these results, we evaluated the possible role of the Notch1 signaling pathway in changes in oligodendroglial cell population during aTf-induced remyelination. In the SVZ of treated animals, the stereotaxic injection of aTf induced an increase in NICD levels 2 and 24 h later. In terms of gene expression, while aTf appeared to succeed in counteracting the effects of LPC in Hes1 and Hes5 levels 24 h after injection, the variations observed in the expression of these genes in LPC-treated animals injected with SS can be attributed to the time-dependent changes inherent to demyelination. In the CC, aTf induced an increase in NICD levels 24 h post-injection, while Hes1 and Hes5 did not show significant modifications. Worth pointing out, in both SVZ and CC, MAG expression was significantly increased by aTf 24 post-injection and remained unchanged by the injection of SS.

In line with these results, aTf induced an increase in F3/contactin levels at 24 h, concomitantly with the increase in MAG gene expression mentioned above. F3/contactin, a glycosyl phosphatidylinositol-anchored neural cell adhesion molecule, is a member of the immunoglobulin superfamily (Revest *et al.* 1999). This protein is a neuronal receptor for the OL-related extracellular matrix glycoprotein tenascin-R through epidermal growth factor-like repeats (Xiao *et al.* 1996). Among other interactions F3/contactin colocalizes and interacts in *cis* with Caspr/Paranodin and in *trans* with glial neurofascin 155 at the paranodal region (Girault and Peles 2002), where axon/OL contact is relevant for myelination to occur. In the OL cell line OLN-93, F3/contactin was found to be a physiological ligand of Notch, promoting, like Jagged1, the nuclear translocation of NICD; F3-induced NICD was, in turn, proven to up-regulate MAG gene expression (Hu *et al.* 2003). In spite of the increase in MAG gene expression in the SVZ, we speculate that MAG mRNA translation will occur in the CC, where OL maturation takes place. It is important to highlight the possible connection between the promyelinating effect of aTf and its differential impact on the expression of Hes genes and MAG: the decrease in Hes5 gene expression may be associated with a decrease in NG2-positive OPCs, thus affecting cell

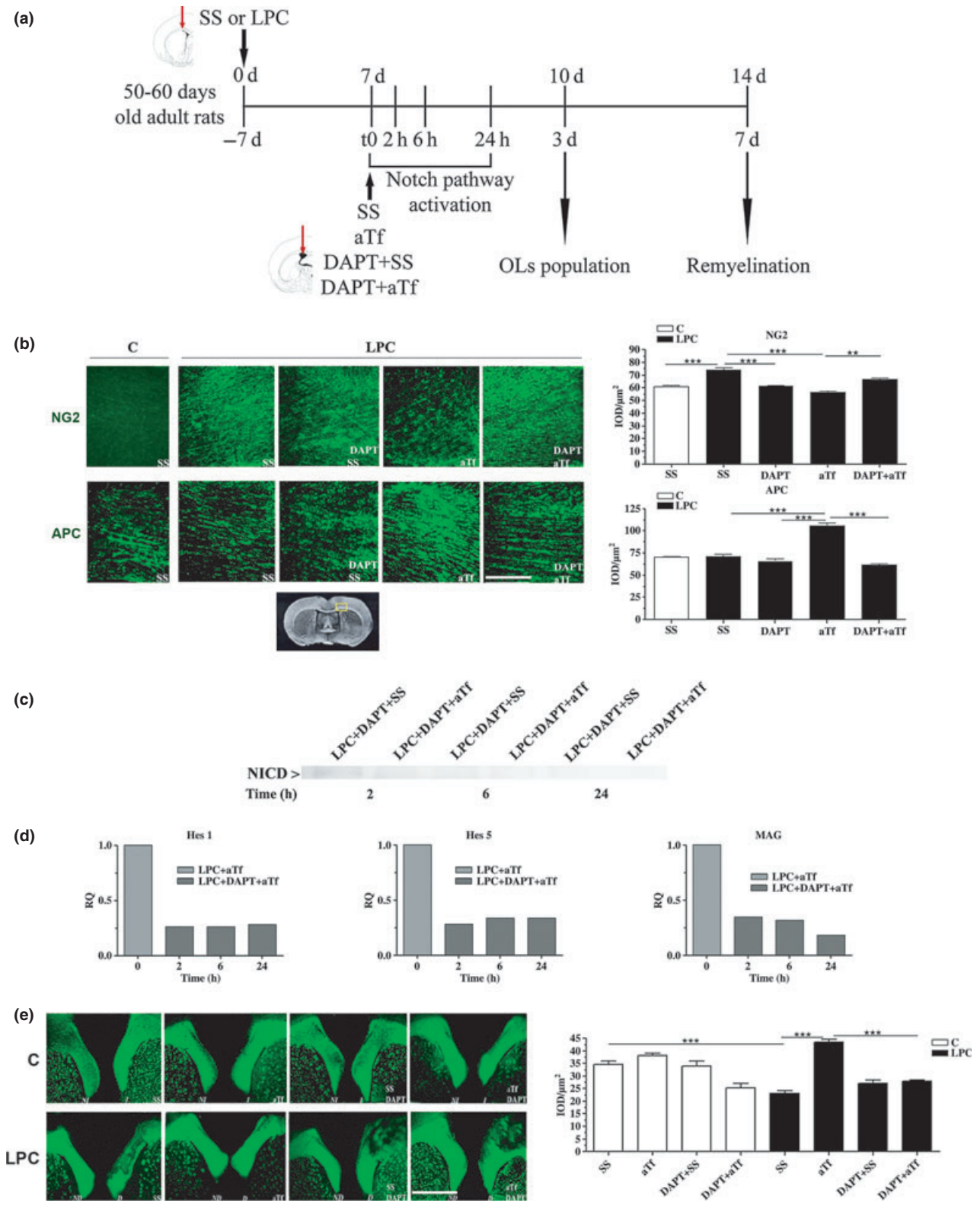
(a)
SS or LPC
0 d
7 d
10 d
14 d
50-60 days
old adult rats
−7 d
t0 2 h 6 h
24 h
3 d
7 d
Notch pathway
activation
SS
aTf
DAPT+SS
DAPT+aTf
OLs population
Remyelination
(b)
C
LPC
NG2
APC
SS
DAPT
aTf
DAPT+aTf
IOD/μm²
(c)
LPC+DAPT+SS
LPC+DAPT+aTf
NICD >
Time (h)
2
6
24
(d)
Hes 1
Hes 5
MAG
LPC+aTf
LPC+DAPT+aTf
RQ
Time (h)
(e)
C
LPC

Fig. 8 The changes in NG2-expressing Oligodendroglial progenitor cells (OPCs) and adenomatous polyposis coli (APC)-expressing differentiated oligodendrocytes (OLs) in corpus callosum (CC) of lysolecithin (LPC)-demyelinated rats, induced by aTf injection, are reversed by the γ-secretase inhibitor. (a) OL populations were evaluated in the CC of control and LPC-treated rats 3 days after the injection of Sterile saline solution (SS) (SS), aTf (aTf), DAPT + SS (DAPT, SS) or DAPT + aTf (DAPT, aTf) into the lateral ventricle. The inhibition of the Notch signaling pathway was evaluated 2, 6, and 24 h after DAPT + SS or DAPT + aTf injection. Remyelination was evaluated 7 days after the injection of SS (SS), aTf (aTf), DAPT + SS (SS, DAPT) or DAPT + aTf (aTf, DAPT) into the lateral ventricle. (b) Immunohistochemistry (IHC) for NG2-expressing OPCs (green) and APC-expressing differentiated OLs (green) in CC of control (C) and LPC-demyelinated animals (LPC) at t0 and 3 days after SS (SS), DAPT + SS (DAPT, SS), aTf (aTf) and DAPT + aTf (DAPT, aTf) injection. Scale bar, 200 μm. After quantifications, values are expressed as the ratio integrated optical density (IOD) units/area (μm^2). Each data point represents the mean ± SEM of three independent experiments performed in triplicate. (c) Western blot analyses for Notch intracellular domain (NICD) in the CC of LPC-demyelinated rats (LPC) 2, 6, and 24 h after the DAPT + SS (LPC + DAPT + SS) or DAPT + aTf (LPC+DAPT+aTf). (d) quantitative real time PCR (RT-PCR) analyses of Notch signaling target genes. Values are expressed as RQ and values for LPC-aTf rats previously injected with DAPT are considered in reference to those of LPC-aTf rats. Results are presented as means ± SEM of three independent experiments performed in triplicate; (e) Myelin staining of CC of control (C), LPC-demyelinated rats (LPC) and LPC-demyelinated rats injected with SS (SS), aTf (aTf), DAPT + SS (SS, DAPT) or DAPT + aTf (aTf, DAPT). Scale bar 200 μm. After quantifications, values are expressed as the ratio IOD units/area (μm^2). Each data point represents the mean ± SEM of three independent experiments performed in triplicate. Significant differences: $^{**}p < 0.01$ and $^{***}p < 0.001$.

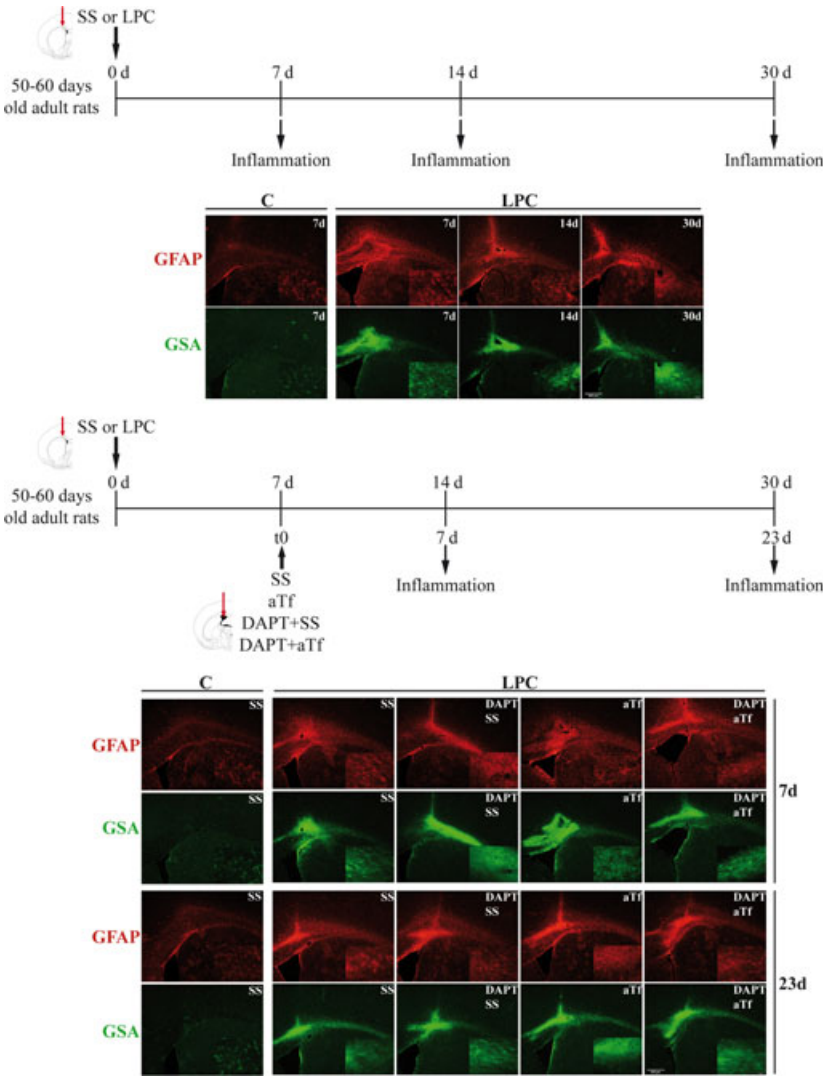

Fig. 9 Inflammatory response in lysolecithin (LPC)-demyelinated rats and during remyelination after aTf and *N*-[*N*-(3,5-Difluorophenalcetyl-L-alanyl)]-*S*-phenylglycine-t-butyl ester (DAPT) treatments. (a) Inflammatory response was evaluated in the Subventricular zone (SVZ) and corpus callosum (CC) 7, 14, or 30 days after Sterile saline solution (SS) or LPC injection into the CC. (b) Astroglial activation was evaluated by glial fibrillary acidic protein (GFAP) (red) and microglial activation was determined by lectin Griffonia simplicifolia (GSA) (green) immunostaining 7 days after SS injection (C) and 7, 14, or 30 days after LPC administration (LPC). Scale bar, 500 μm. Insets show higher magnification of the injection site. Scale bar 50 μm. (c) Inflammatory response was evaluated in the SVZ and CC of control (C) and LPC-demyelinated rats (LPC) 7 and 23 days after SS, aTf, DAPT + SS, and DAPT + aTf injection into the lateral ventricle. (d) Astroglial activation was evaluated by GFAP (red) and microglial activation was determined by GSA (green) immunostaining in CC and SVZ of control (C) and LPC-demyelinated animals (LPC) 7 and 23 days after SS (SS), aTf (aTf), DAPT + SS (DAPT, SS) or DAPT + aTf (DAPT, aTf). Scale bar 500 μm. Insets show higher magnification of the injection site. Scale bar 50 μm.

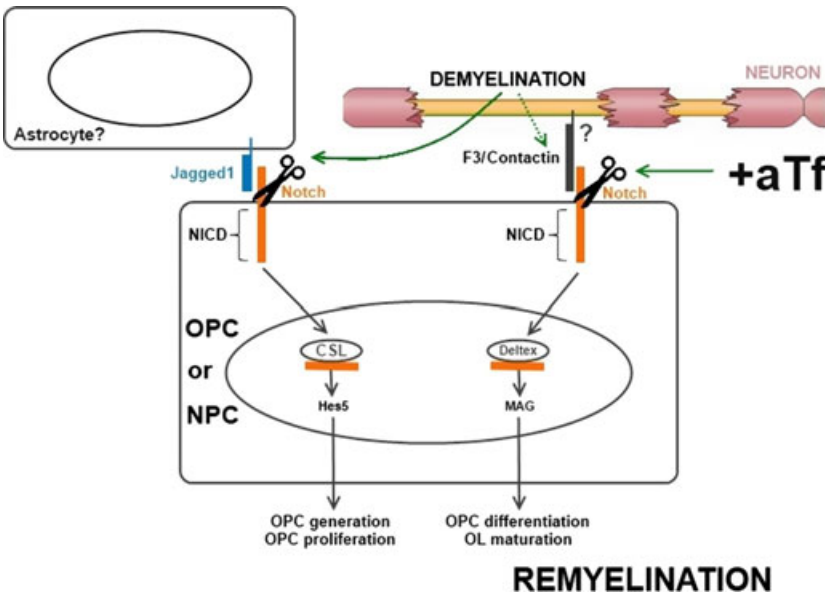

Fig. 10 As an early consequence of demyelination, the expression of Jagged1 is induced in a cell type still to be characterized both in the Subventricular zone (SVZ) and corpus callosum (CC). In turn, Jagged1 might trigger Notch signaling pathway activation, generating Notch intracellular domain (NICD) release and inducing Hes5 expression. This gene's expression might then promote Oligodendroglial progenitor cell (OPC) generation from neural progenitor cells (NPCs) present in the SVZ or the proliferation of OPCs already present both in the SVZ and CC. The administration of aTf induces F3/contactin expression, probably in the axon. In turn, F3/contactin might trigger Notch activation and NICD release, inducing the expression of myelin-associated glycoprotein (MAG).

proliferation, while the increase in MAG expression may be associated with the maturation of OLs.

In terms of astrocytic and microglial participation, it is well known that peripherally derived macrophages and the microglia resident in the CNS play an important role in the remyelination process. These cells are implicated in CNS autoimmunity through the secretion of toxic molecules (Banati *et al.* 1993) and the presentation of antigens to cytotoxic lymphocytes (Cash *et al.* 1993), but they also favor the remyelination process via the phagocytosis of myelin debris (Kotter *et al.* 2006; Ruckh *et al.* 2012) and secretion of growth factors (Kotter *et al.* 2005). In this context, we evaluated the possible changes in microglia and astrocytes as a consequence of demyelination and during remyelination induced by aTf and in the presence of the γ-secretase inhibitor. We found microglial activation and GFAP-positive astrocytes in the CC ipsilateral to the LPC injection regardless of treatment or time point studied. In turn, Miron *et al.* (Miron *et al.* 2013) have recently found a switch from M1 to M2 functional phenotypes in both resident microglia and peripherally derived macrophages during the remyelination of LPC-induced demyelinated lesions. Nevertheless, as we measured total microglial populations and did not analyze M1 and M2 phenotypes, our results are not in conflict with these findings and may even be in agreement.

Considering these results, we propose that, as a consequence of demyelination, Jagged1 triggers Notch activation in NPCs and OPCs present in the SVZ. Hes5 gene expression in these cells mediates both OPC proliferation and the commitment of NPCs toward oligodendroglial progeny. On the other hand, in the CC, Notch activation in OPCs promotes Hes-mediated cell proliferation. In our hypothesis, demyelination could trigger the axonal expression of F3/contactin to induce OL maturation by up-regulating MAG gene expression. aTf would then accelerate the process, promoting remyelination. Furthermore, considering that aTf induced an increase in F3/contactin and NICD 24 h post-injection, concomitantly with an increase in MAG gene expression, and that DAPT injection reversed the remyelination induced by aTf in LPC-demyelinated animals, we propose that Notch signaling is involved, at least in part, in the promyelinating effect of aTf (Fig. 10).

Evidence of the participation of Notch signaling in the demyelination/remyelination process will help further understand demyelinating disorders such as MS and the use of aTf should be taken into consideration as a possible therapeutic intervention.

Acknowledgements

Supported by grants from ANPCyT (PICT 15-25408), University of Buenos Aires (20020090100281) and CONICET (PIP830), Argentina. We are very thankful to Dr. Julieta Kopka for her skilful support in Real Time PCR determinations. The authors declare no conflict of interest.

References

Adamo A. M., Paez P. M., Escobar Cabrera O. E., Wolfson M., Franco P. G., Pasquini J. M. and Soto E. F. (2006) Remyelination after cuprizone-induced demyelination in the rat is stimulated by apotransferrin. *Exp. Neurol.* **198**, 519–529.

Artavanis-Tsakonas S., Rand M. D. and Lake R. J. (1999) Notch signaling: cell fate control and signal integration in development. *Science* **284**, 770–776.

Banati R. B., Gehrmann J., Schubert P. and Kreutzberg G. W. (1993) Cytotoxicity of microglia. *Glia* **7**, 111–118.

Bradford M. M. (1976) A rapid and sensitive method for the quantitation of microgram quantities of protein utilizing the principle of protein-dye binding. *Anal. Biochem.* **72**, 248–254.

Cash E., Zhang Y. and Rott O. (1993) Microglia present myelin antigens to T cells after phagocytosis of oligodendrocytes. *Cell. Immunol.* **147**, 129–138.

Chari D. M. and Blakemore W. F. (2002) Efficient recolonisation of progenitor-depleted areas of the CNS by adult oligodendrocyte progenitor cells. *Glia* **37**, 307–313.

Cui X. Y., Hu Q. D., Tekaya M. *et al.* (2004) NB-3/Notch1 pathway via Deltex1 promotes neural progenitor cell differentiation into oligodendrocytes. *J. Biol. Chem.* **279**, 25858–25865.

Escobar Cabrera O. E., Bongarzone E. R., Soto E. F. and Pasquini J. M. (1994) Single intracerebral injection of apotransferrin in young rats induces increased myelination. *Dev. Neurosci.* **16**, 248–254.

Escobar Cabrera O. E., Zakin M. M., Soto E. F. and Pasquini J. M. (1997) Single intracranial injection of apotransferrin in young rats increases the expression of specific myelin protein mRNA. *J. Neurosci. Res.* **47**, 603–608.

Escobar Cabrera O. E., Soto E. F. and Pasquini J. M. (2000) Myelin membranes isolated from rats intracranially injected with apotransferrin are more susceptible to in vitro peroxidation. *Neurochem. Res.* **25**, 87–93.

Espinosa de los Monteros A., Pena L. A. and de Vellis J. (1989) Does transferrin have a special role in the nervous system? *J. Neurosci. Res.* **24**, 125–136.

Espinosa de los Monteros A., Kumar S., Zhao P., Huang C. J., Nazarian R., Pan T., Scully S., Chang R. and de Vellis J. (1999) Transferrin is an essential factor for myelination. *Neurochem. Res.* **24**, 235–248.

Espinosa-Jeffrey A., Kumar S., Zhao P. M., Awosika O., Agbo C., Huang A., Chang R. and De Vellis J. (2002) Transferrin regulates transcription of the MBP gene and its action synergizes with IGF-1 to enhance myelinogenesis in the md rat. *Dev. Neurosci.* **24**, 227–241.

Franklin R. J. (2002) Why does remyelination fail in multiple sclerosis? *Nat. Rev. Neurosci.* **3**, 705–714.

Franklin R. J. and Ffrench-Constant C. (2008) Remyelination in the CNS: from biology to therapy. *Nat. Rev. Neurosci.* **9**, 839–855.

Gao F., Zhang Q., Zheng M. H. *et al.* (2009) Transcription factor RBP-J-mediated signaling represses the differentiation of neural stem cells into intermediate neural progenitors. *Mol. Cell. Neurosci.* **40**, 442–450.

Girault J. A. and Peles E. (2002) Development of nodes of Ranvier. *Curr. Opin. Neurobiol.* **12**, 476–485.

Hu Q. D., Ang B. T., Karsak M. *et al.* (2003) F3/contactin acts as a functional ligand for Notch during oligodendrocyte maturation. *Cell* **115**, 163–175.

Jeffery N. D. and Blakemore W. F. (1997) Locomotor deficits induced by experimental spinal cord demyelination are abolished by spontaneous remyelination. *Brain* **120**(Pt 1), 27–37.

John G. R., Shankar S. L., Shafit-Zagardo B., Massimi A., Lee S. C., Raine C. S. and Brosnan C. F. (2002) Multiple sclerosis: re-expression of a developmental pathway that restricts oligodendrocyte maturation. *Nat. Med.* **8**, 1115–1121.

Jurynczyk M., Jurewicz A., Bielecki B., Raine C. S. and Selmaj K. (2008) Overcoming failure to repair demyelination in EAE: gamma-secretase inhibition of Notch signaling. *J. Neurol. Sci.* **265**, 5–11.

Kaplan M. S. and Hinds J. W. (1980) Gliogenesis of astrocytes and oligodendrocytes in the neocortical grey and white matter of the adult rat: electron microscopic analysis of light radioautographs. *J. Comp. Neurol.* **193**, 711–727.

Kaur C. and Ling E. A. (1991) Study of the transformation of amoeboid microglial cells into microglia labelled with the isolectin Griffonia simplicifolia in postnatal rats. *Acta Anat.* **142**, 118–125.

Kopan R. and Ilagan M. X. (2009) The canonical Notch signaling pathway: unfolding the activation mechanism. *Cell* **137**, 216–233.

Kotter M. R., Zhao C., van Rooijen N. and Franklin R. J. (2005) Macrophage-depletion induced impairment of experimental CNS remyelination is associated with a reduced oligodendrocyte progenitor cell response and altered growth factor expression. *Neurobiol. Dis.* **18**, 166–175.

Kotter M. R., Li W. W., Zhao C. and Franklin R. J. (2006) Myelin impairs CNS remyelination by inhibiting oligodendrocyte precursor cell differentiation. *J. Neurosci.* **26**, 328–332.

Kreutzberg G. W. (1996) Microglia: a sensor for pathological events in the CNS. *Trends Neurosci.* **19**, 312–318.

Laemmli U. K. (1970) Cleavage of structural proteins during the assembly of the head of bacteriophage T4. *Nature* **227**, 680–685.

Lassmann H., Bruck W. and Lucchinetti C. F. (2007) The immunopathology of multiple sclerosis: an overview. *Brain Pathol.* **17**, 210–218.

Liebetanz D. and Merkler D. (2006) Effects of commissural de- and remyelination on motor skill behaviour in the cuprizone mouse model of multiple sclerosis. *Exp. Neurol.* **202**, 217–224.

Ludwin S. K. (1978) Central nervous system demyelination and remyelination in the mouse: an ultrastructural study of cuprizone toxicity. *Lab. Invest.* **39**, 597–612.

Lutolf S., Radtke F., Aguet M., Suter U. and Taylor V. (2002) Notch1 is required for neuronal and glial differentiation in the cerebellum. *Development* **129**, 373–385.

Marta C. B., Paez P., Lopez M., Pellegrino de Iraldi A., Soto E. F. and Pasquini J. M. (2003) Morphological changes of myelin sheaths in rats intracranially injected with apotransferrin. *Neurochem. Res.* **28**, 101–110.

Matsushima G. K. and Morell P. (2001) The neurotoxicant, cuprizone, as a model to study demyelination and remyelination in the central nervous system. *Brain Pathol.* **11**, 107–116.

McCarthy G. F. and Leblond C. P. (1988) Radioautographic evidence for slow astrocyte turnover and modest oligodendrocyte production in the corpus callosum of adult mice infused with 3H-thymidine. *J. Comp. Neurol.* **271**, 589–603.

Miller R. H. and Mi S. (2007) Dissecting demyelination. *Nat. Neurosci.* **10**, 1351–1354.

Miron V. E., Boyd A., Zhao J. W. *et al.* (2013) M2 microglia and macrophages drive oligodendrocyte differentiation during CNS remyelination. *Nat. Neurosci.* **16**, 1211–1218.

Nicolay D. J., Doucette J. R. and Nazarali A. J. (2007) Transcriptional control of oligodendrogenesis. *Glia* **55**, 1287–1299.

Oberhammer F., Fritsch G., Schmied M., Pavelka M., Printz D., Purchio T., Lassmann H. and Schulte-Hermann R. (1993) Condensation of the chromatin at the membrane of an apoptotic nucleus is not associated with activation of an endonuclease. *J. Cell Sci.* **104**(Pt 2), 317–326.

Park H. C. and Appel B. (2003) Delta-Notch signaling regulates oligodendrocyte specification. *Development* **130**, 3747–3755.

Prineas J. W. and Connell F. (1979) Remyelination in multiple sclerosis. *Ann. Neurol.* **5**, 22–31.

Revest J. M., Faivre-Sarrailh C., Schachner M. and Rougon G. (1999) Bidirectional signaling between neurons and glial cells via the F3 neuronal adhesion molecule. *Adv. Exp. Med. Biol.* **468**, 309–318.

Rowitch D. H. (2004) Glial specification in the vertebrate neural tube. *Nat. Rev. Neurosci.* **5**, 409–419.

Ruckh J. M., Zhao J. W., Shadrach J. L., van Wijngaarden P., Rao T. N., Wagers A. J. and Franklin R. J. (2012) Rejuvenation of regeneration in the aging central nervous system. *Cell Stem Cell* **10**, 96–103.

Saleh M. C., Espinosa de los Monteros A., de Arriba Zerpa G. A. *et al.* (2003) Myelination and motor coordination are increased in transferrin transgenic mice. *J. Neurosci. Res.* **72**, 587–594.

Suzuki K. and Kikkawa Y. (1969) Status spongiosus of CNS and hepatic changes induced by cuprizone (biscyclohexanone oxalyldihydrazone). *Am. J. Pathol.* **54**, 307–325.

Tagami S., Okochi M., Yanagida K. *et al.* (2008) Regulation of Notch signaling by dynamic changes in the precision of S3 cleavage of Notch-1. *Mol. Cell. Biol.* **28**, 165–176.

Taylor M. K., Yeager K. and Morrison S. J. (2007) Physiological Notch signaling promotes gliogenesis in the developing peripheral and central nervous systems. *Development* **134**, 2435–2447.

Thomas J. L., Spassky N., Perez Villegas E. M., Olivier C., Cobos I., Goujet-Zalc C., Martinez S. and Zalc B. (2000) Spatiotemporal development of oligodendrocytes in the embryonic brain. *J. Neurosci. Res.* **59**, 471–476.

Timsit S., Martinez S., Allinquant B., Peyron F., Puelles L. and Zalc B. (1995) Oligodendrocytes originate in a restricted zone of the embryonic ventral neural tube defined by DM-20 mRNA expression. *J. Neurosci.* **15**, 1012–1024.

Wang S., Sdrulla A. D., diSibio G., Bush G., Nofziger D., Hicks C., Weinmaster G. and Barres B. A. (1998) Notch receptor activation inhibits oligodendrocyte differentiation. *Neuron* **21**, 63–75.

Warf B. C., Fok-Seang J. and Miller R. H. (1991) Evidence for the ventral origin of oligodendrocyte precursors in the rat spinal cord. *J. Neurosci.* **11**, 2477–2488.

Xiao Z. C., Taylor J., Montag D., Rougon G. and Schachner M. (1996) Distinct effects of recombinant tenascin-R domains in neuronal cell functions and identification of the domain interacting with the neuronal recognition molecule F3/11. *Eur. J. Neurosci.* **8**, 766–782.